

NUMERICAL CALCULATIONS OF THE EFFECTS OF SPACE CHARGE*
ON SIX DIMENSIONAL BEAM DYNAMICS IN PROTON LINEAR ACCELERATORS

R. Chasman
Brookhaven National Laboratory

1. Introduction

In a high current low energy proton linac, repulsive space charge forces become comparable to transverse quadrupole and longitudinal rf focussing forces. Consequently the effects of space charge have to be included in studies of beam dynamics for the design of such machines. In the past, various aspects of the behavior of a high current proton linac beam have primarily been treated analytically. As early as 1959 Kapchinskij and Vladimirskij¹ calculated the effects of space charge on the transverse motion assuming that the beam is a uniformly charged infinitely long elliptical cylinder. In particular they pointed out the importance of a transversely matched beam for maximum transmission of current. Kapchinskij and Kronrod² and also Morton³ examined the reduction due to space charge in the longitudinal acceptance of a linac. In the last few years additional analytical calculations of the effects of space charge on linac beam dynamics have been published. The longitudinal motion was treated by Gluckstern⁴, by Lapostolle⁵ and by Nishikawa⁶ and a space charged modified stability diagram for the transverse motion was calculated by Ohnuma⁷. All these analytical studies are based on the assumption of self-consistent uniform charge distributions (either an ellipsoid or an infinitely long elliptical cylinder) which lead to linear forces and linear separable equations of motion. These distributions, as pointed out by Kapchinskij and Vladimirskij¹ and later by Lapostolle⁸ and by Ohnuma⁹, are highly unrealistic in 4 or 6 dimensional phase space. Furthermore, they exclude effects of longitudinal-transverse and transverse-transverse coupling which lead to two dimensional emittance growth. It therefore seemed desirable to carry out 6 dimensional numerical computations which can take into account space charge effects without the limitations imposed on previous analytical work. It is the purpose of this paper to describe such calculations and to report on some of their results.

2. Computer Program

Extensive six dimensional linac orbit computations in the zero space charge approximation have been performed earlier in several laboratories. Particle motion codes used for these calculations are very similar and based on identical assumptions:

Acceleration takes place over an infinitesimally small interval in the middle of the gap be-

* Work performed under the auspices of the U. S. Atomic Energy Commission.

tween drift tubes. The transit time factor is a function not only of cell number but also of particle energy and distance from the linac axis. An abrupt change in phase is introduced in the middle of the gap to guarantee conservation of longitudinal phase space area (Promé approximation).

For the calculations reported below space charge forces have been incorporated into such a computer program in the following way: Each particle is assumed to be a small uniformly charged sphere whose radius is determined by the nearby particle density. The volumes and charges of all the spheres add up to those of the beam bunch. (Neighboring bunches are not considered.) The total space charge force acting on a point in the beam is the sum of the forces from all spheres. Coherent and incoherent image forces in the drift tube walls and in the gap between drift tubes are neglected. No beam loading effects are considered. A detailed outline of the space charge modified program has recently been prepared as a Brookhaven internal report¹⁰. Somewhat different models have been used in other laboratories to describe space charge forces.

3. Choice of Initial Conditions

As mentioned in the Introduction, Kapchinskij and Vladimirskij¹ long ago recognized the importance of matching the beam transversely. Because the longitudinal dimensions of the beam bunch in the beginning of a conventional linac is of the same order of magnitude as the transverse dimensions, it was decided to try to match the beam both longitudinally and transversely. The initial beam dimensions were chosen on the basis of this requirement. Assuming that the beam bunch is a uniformly charged ellipsoid one can write down the non-relativistic beam envelope equations taking the smooth approximation for the transverse motion:

$$\frac{d^2 a}{dn^2} + k_t^2 \beta^2 \lambda^2 \cdot a - \frac{p^2}{a^3} = \frac{\mu \cdot \left(1 - f \left(\frac{c}{a}\right)\right)}{2ac} \quad (1a)$$

* At Los Alamos, a linac motion code called Parmilla, has been modified to include space charge forces in the form of either ring-ring or point-point interactions. Some calculations have already been performed with both versions of this program¹¹. Similar codes taking into account space charge forces also exist at Chalk River¹² and at CERN¹³.

$$\frac{d^2c}{dn^2} + k_\ell^2 \beta^2 \lambda^2 \cdot c - \frac{Q^2}{3} = \frac{\mu \cdot f(\frac{c}{a})}{a^2} \quad (1b)$$

$$\mu = \frac{90Q_0 \cdot eI\lambda^3}{m_0}$$

Here $dn = ds/\beta\lambda$ (λ is the rf wavelength, s is the distance along the linac axis, both in meters).

a is the average beam radius in meters. ($a = \sqrt{a_x a_y}$ where $2a_x$ and $2a_y$ are the widths of the beam bunch in the x and y directions. At a symmetry point in an x -focussing and y -defocussing quadrupole magnet $a_x/a_y = \psi$, where ψ can be obtained from the stability diagram.)

$2c$ is the length of the bunch in meters.

k_t is the wavenumber in meter⁻¹ of the transverse particle oscillations in the zero space charge approximation.

k_ℓ is the wavenumber in meter⁻¹ of the longitudinal particle oscillations in the zero space charge approximation.

P is the area of the beam in $\pi \cdot \text{meter}^2$ in the a , da/dn space.

Q is the area of the beam in $\pi \cdot \text{meter}^2$ in the c , dc/dn space (it is proportional to the conventional longitudinal emittance in $\Delta\gamma\text{-}\Delta\phi$ space).

I is the current in amperes.

m_0 is the proton rest mass in eV.

$f(\frac{c}{a})$ is a form factor for the ellipsoid and can be approximated by

$$\frac{a}{3c} \text{ for } 1 < \frac{c}{a} < 5 .$$

For matched conditions

$$\frac{d^2a}{dn^2} \cong 0 \text{ and } \frac{d^2c}{dn^2} \cong 0 .$$

One then gets two simultaneous equations in a and c :

$$k_t^2 \beta^2 \lambda^2 a - \frac{P^2}{3} = \frac{\mu \left(1 - f\left(\frac{c}{a}\right)\right)}{2ac} \quad (2a)$$

$$k_\ell^2 \beta^2 \lambda^2 c - \frac{Q^2}{3} = \frac{\mu \cdot f\left(\frac{c}{a}\right)}{a^2} \quad (2b)$$

k_t and k_ℓ are given by machine parameters:

$$k_t = \frac{\mu_{SF}}{2\beta\lambda}$$

where μ_{SF} is the phase advance of the transverse particle oscillation per magnet period for zero current (assuming +-+ quadrupole configuration)

$$k_\ell = \left[\frac{2\pi e E_0 T \sin(|\varphi_s|)}{m_0 \lambda \beta^3} \right]^{\frac{1}{2}}$$

where E_0 is the average electric field in V/m

T is the transit time factor

φ_s is the synchronous phase.

Assuming a fixed energy spread, $\Delta\gamma_i$, at injection (which is compatible with results from recent space charge calculations on buncher design)¹⁴, one gets $Q \sim c \cdot \Delta\gamma_i$ and one can solve equations (2a) and (2b) for a and c for different values of I and P .

In order to accelerate the beam without losses, a/ψ^* , the maximum transverse beam dimension, has to be considerably smaller than the bore radius so that the beam will not strike the bore even after transverse beam growth. The longitudinal dimension of the beam bunch, c , is equal to

$$\frac{\beta\lambda \Delta\phi_{\max}}{2\pi}$$

($\Delta\phi_{\max}$ is half the phase spread of the beam) and $\pm \Delta\phi_{\max}$ has to be within the phase acceptance of the machine if no part of the beam is to be lost longitudinally. The region of phase acceptance is roughly estimated as $-\varphi_s \leq \Delta\phi \leq 2\varphi_s$. Figure 1 shows values of a and c obtained from equations (2a) and (2b) for different values of I , the beam current, and for different initial quadrupole gradients. Regions of phase and radial acceptance are also indicated. All other machine parameters are those of the new BNL 200 MeV injector linac. (These are indicated in Fig. 1.) It was assumed that the transverse emittance is $I \cdot 22.5 \pi \text{ cm mrad}$, where I is in amperes. These emittances have been obtained from recently developed preinjector systems^{15,16,17}. Figure 2 shows a and c as functions of I for various other initial transverse emittances and for an initial quadrupole gradient of 9.15 kG/cm.

For each computer run a and c were obtained from equations (2a), (2b), and particles were distributed in 6 dimensional phase space in the following way: A 4 dimensional hyperellipsoid in

* Results in Ref. 7 indicate that ψ can be taken from the zero space charge approximation stability diagram.

x - p_x - y - p_y space with semi-axis $x_{\max} = a/\psi$, $(p_x)_{\max} = P/a/\psi$, $y_{\max} = a/\psi$ and $(p_y)_{\max} = P/\psi/a$ was randomly filled. In longitudinal phase space an ellipse with semi-axis $(\Delta\phi)_{\max} = c \cdot 2\pi/\beta\lambda$ and $\Delta\gamma_i = 0.000021$ (corresponding to 0.020 MeV energy spread) was also randomly populated. No correlation was introduced between transverse and longitudinal coordinates and approximately 500 particles were used to fill out the six dimensional volume specified by x_{\max} , $(p_x)_{\max}$, y_{\max} , $(p_y)_{\max}$, $\Delta\phi_{\max}$ and $\Delta\gamma_i$. The described six dimensional input distribution does not yield a uniform charge distribution in physical three dimensional space. Integrating over p_x , p_y and $\Delta\gamma$ one gets

$$\rho(x, y, \Delta\phi) \sim (1-r^2) \sqrt{1 - \frac{\Delta\phi^2}{\Delta\phi_{\max}^2}}$$

where $x = x_{\max}r \cos\theta$, $y = y_{\max}r \sin\theta$ and $0 \leq r \leq 1$.

4. Results

a. Limiting Currents

For an initial quadrupole gradient of 9.15 kG/cm computer runs were made up to 10 MeV for different currents in the range 50-500 mA.

Figure 3 shows output versus input current and also the longitudinal losses in percent as function of input current. Theoretical fractional longitudinal losses estimated roughly from

$$\frac{\Delta\phi_{\max} - \phi_s}{2\Delta\phi_{\max}}$$

are also plotted for comparison. The computer program indicated no radial losses. As can be seen from the curves in Fig. 1 which were derived from the ellipsoidal model, some longitudinal losses could be expected for currents above 100 mA (for which $\Delta\phi_{\max} > \phi_s$) while radial losses should be small.

Additional runs with 50, 100 and 200 mA were made for an initial quadrupole gradient of 5.63 kG/cm. Figure 4 shows output current and radial losses in percent as function of input current. No longitudinal losses were obtained. Figure 1 (ellipsoidal model) predicts that particles should be lost radially in this case.

b. Beam Envelope Oscillations

As mentioned in Section 2, beam dimensions at injection were chosen in an effort to match the beam both longitudinally and transversely, i.e., to reduce beam envelope oscillations. Figure 5 shows the average radius, $r_{av} = \sqrt{x_{\max} \cdot y_{\max}}$, of a 100 mA beam and its phase spread $\Delta\phi_{\max}$ as function of drift tube number up to 10 MeV. r_{av} and $\Delta\phi_{\max}$ were obtained from an output routine which calculates rms values of particle coordinates. The longitudinal and transverse beam envelope oscillations of an initially transversely mismatched beam are also shown for comparison in Fig. 5. The

graphs show that the beam envelopes of the matched beam oscillate slightly about smoothly varying curves (drawn in with dotted lines). The amplitudes of these oscillations are within 10% of the average values of r_{av} and $\Delta\phi_{\max}$. Similar results were obtained for other currents in the range 50-500 mA. This implies that the match is indeed reasonably good in spite of the assumptions of uniform charge density, linear forces and smoothed transverse motion which were used in the envelope equations (1) and (2) to obtain matched input conditions but which were abandoned in the computer program.

c. Emittance Growth

In all computer runs the areas which the beam occupies in the transverse and longitudinal phase space planes were calculated in each drift tube by a rms method. Results from these computations show that the longitudinal phase space area is constant to within 15% but that there is considerable increase in transverse emittance. The nature of this transverse emittance growth was further investigated in the following way:

Since magnet misalignment errors and nonlinearities are not included in the computer program an increase in transverse emittance can be caused primarily by two effects:

I. Longitudinal-transverse coupling through the rf field in the gap between drift tubes.

II. Longitudinal-transverse and transverse-transverse coupling from non-linear space charge forces.

In order to separate these two possible causes for transverse emittance growth, changes were made in the computer program which removed the coupling between the transverse and longitudinal motion, introduced by the rf field in the gap. This can be done by making the transit time factor and the rf defocussing force in the gap functions of cell number only and hence excluding their dependence on particle coordinates. (In this case the Promé correction is zero.) The transverse emittances were recomputed under otherwise unchanged conditions. Results obtained with and without rf coupling for 100 mA between 0.750 MeV and 30 MeV are shown in Fig. 6. Figure 7 shows the particle distributions in the x - p_x and y - p_y planes at 0.750 and 10 MeV in the run with rf coupling. Comparison between these distributions at 0.750 MeV and 10 MeV confirms the magnitude of transverse emittance growth shown in Fig. 6. As can easily be recognized from Fig. 6 the curves obtained with and without longitudinal-transverse coupling through the rf field are very similar and one can hardly blame the transverse emittance growth on this coupling effect. In order to minimize space charge forces computer runs were also made for 1 mA and otherwise identical conditions. Values for transverse emittances were again calculated and are also plotted in Fig. 6. They show no significant increase between 0.750 MeV and 10 MeV. One can therefore conclude that the origin of the transverse emittance growth most probably lies

in non-linear space charge forces. As can be seen from Fig. 6 the transverse beam blow-up occurs almost entirely below 10 MeV.

Additional computer runs were made to see in what way the increase in transverse emittance depends on beam and machine parameters:

Figure 8 shows the normalized transverse emittance obtained at 10 MeV for 100 mA and various values of initial normalized emittance. Results indicate that the transverse emittance blow-up grows rapidly with decreasing initial emittance and there seems to be a lower limit to the normalized emittance at 10 MeV. The dotted line represents the situation for constant normalized emittance.

Detailed results of the runs with 0.009π cm-mrad initial normalized emittance are shown in Fig. 9. Transverse and longitudinal beam envelopes and transverse phase space areas are plotted as functions of drift tube number. The corresponding beam brightness (defined as $B = I \cdot 10^6 / \pi^2 \epsilon^2$ in mA/cm²rad², $\epsilon \cdot \pi =$ normalized emittance) is 2.5×10^{11} or 100 times larger than that obtained from recently developed preinjector systems.

Results shown in Fig. 8 suggest that the observed transverse emittance blow-up depends strongly on the brightness of the beam. Computer runs were made for different currents but constant brightness and the fractional increases in normalized emittance at 10 MeV obtained from these runs are shown in Fig. 10.

Values for the fractional increase in normalized emittance at 10 MeV deduced from runs with different currents and initial emittances are shown in Fig. 11 as function of brightness.

The x - p_x emittance versus drift tube number of a 100 mA transversely mismatched beam (see Fig. 5) is shown in Fig. 12 together with that of a 100 mA matched beam. Results indicate that the emittance blow-up becomes considerably worse if the beam is not matched.

Another particle distribution in x - p_x - y - p_y space was also tried to find out whether the transverse emittance growth found in the present calculations is sensitive to the input conditions chosen in the program. The uniform density distribution in x - p_x - y - p_y space was replaced by a distribution which was gaussian in both transverse phase space planes separately. Very similar results were obtained for the increase in transverse emittance up to 10 MeV. Runs which were repeated with fewer particles also yielded consistent results.

The dependence of the fractional increase in transverse emittance on initial quadrupole gradient, G_1 , is shown in Fig. 13 for a 100 mA beam. The deterioration of transverse beam quality which was obtained for $G_1 = 5.63$ kG/cm and was accompanied by radial losses is not surprising if one considers that net focussing forces are small for

this initial quadrupole gradient. However, it is not immediately clear why going to much higher gradients (such as 12.67 kG/cm) fails to improve the situation. This might be connected with the fact that the space charge density increases with increasing gradient and the non-linear space charge forces become even more important.

d. Phase Damping and Energy Spread

Previous analytical^{4,5,6} and numerical calculations¹⁸ on the effect of space charge on the longitudinal motion have suggested that phase damping goes as β^{-p} where $1/2 < p < 3/4$. The exponent p approaches $1/2$ for very strong space charge forces. In all those calculations the beam cross section was assumed to stay constant during acceleration.

Results from the present computer calculations indicate that the phase spread of the beam decreases as $\beta^{-3/4}$ even for strong space charge forces. However, as can be seen in Figs. 3 and 6 the transverse beam cross section does not remain fixed but increases with the energy of the beam. (The increase in beam cross section is determined by the amount of transverse emittance growth and also by the magnet law, i.e., quadrupole gradient versus drift tube number.) This results in weaker longitudinal space charge forces and faster phase damping.

The energy spread of the beam bunch was also calculated in each drift tube by an rms method. No significant deviation was found from the $\sim \beta^{+3/4}$ law expected for the increase of energy spread with acceleration in the zero space charge linear theory approximation. This is consistent with $\beta^{-3/4}$ phase damping and constant longitudinal phase space area.

5. Discussion of Results

a. The numerical computations which have been described in this paper indicate that the ellipsoidal model succeeds fairly well in predicting the current which can be accelerated through a particular linac and also in dictating matched input conditions for the beam. However, as was pointed out in the Introduction, the assumption of a uniformly charged ellipsoid (which leads to linear space charge forces) does not account for any emittance growth. In an effort to explain semi-quantitatively the emittance blow-up which was observed for bright beams in the present calculations the following crude estimates can be obtained from the matched beam envelope equations (2a) and (2b). These equations can be rewritten as

$$k_t'^2 \cdot \beta^2 \lambda^2 = \frac{P^2}{a} \quad (3a)$$

$$k_c'^2 \beta^2 \lambda^2 = \frac{Q^2}{c} \quad (3b)$$

where

$$k_t'^2 = k_t^2 - \frac{\mu \left(1 - \frac{a}{3c}\right)}{2a^2 c \beta^2 \lambda^2}$$

$$k_l'^2 = k_l^2 - \frac{\mu}{3ac^2 \beta^2 \lambda^2}$$

The wave numbers k_t' and k_l' are for the single particle transverse and longitudinal oscillations in the presence of space charge forces. In the limit of large space charge forces, neglecting a compared to $3c$, one obtains from equations (3a) and (3b)

$$k_t'^2 \sim \frac{p^2}{I^{4/3}} \quad (4)$$

for beams of large brightness. The brightness B is proportional to I/p^2 and hence $k_t'^2$ is not far from being proportional to $1/B$.

In terms of the strong focussing stability diagram (where $\mu_{SF} = 2k_t' \beta \lambda$, if one includes space charge forces) this means that for very bright beams, regardless of machine parameters, one operates close to $\mu_{SF} = 0$ or $\cos \mu_{SF} = 1$, one of the two stability limits. Large emittance growth might be expected, then, for any existing coupling effects. Analytical calculations are needed to determine the detailed nature of the observed coupling.

b. Results on the transverse emittance blow-up, both those shown in Fig. 6 and others which were obtained from additional computer runs, point to the relative unimportance of the longitudinal-transverse coupling through the rf field in the gap. Analytical and numerical studies^{19,20,21,22} of this effect have been made earlier in the zero space charge approximation and showed that it causes appreciable increase in transverse emittance contrary to the findings in this paper. However, these calculations were made with border particles in both transverse and longitudinal phase space planes and hence yielded results which should be interpreted as values for beam growth of the "worst" particles. Results given in this paper have been obtained from calculations in which particles were chosen from the entire interior of the longitudinal and transverse phase space ellipses and the areas which the particles occupy in the two dimensional phase space planes were evaluated by rms calculations. By doing so, one takes also into account particles whose amplitude decreases, thus leading to greatly reduced values of the rms beam growth.

6. Summary

Six dimensional linac orbit calculations, performed with a computer program which was designed to include space charge forces in a perfect linac, have suggested the following conclusions:

a. A simple reliable prescription has been found to match the beam to both the longitudinal

and transverse admittances of the linac. The resultant beam envelope oscillations remain quite small during the acceleration.

b. Matched beams with currents up to several hundred milliamperes can be accelerated through the linac using measured characteristics of recently developed preinjectors and high initial quadrupole gradients.

c. There is considerable transverse emittance growth in beams with a brightness (defined in Section 4c) of 10^9 and higher. This appears to be caused by non-linear space charge forces.

Acknowledgments

The author expresses her sincere gratitude to Professor R. L. Gluckstern for his advice and interest throughout this work, and is indebted to Drs. J. Claus and Th. J. M. Sluyters for valuable discussions.

References

1. I. M. Kapchinskij and V. V. Vladimirskij, Conference on High Energy Accelerators and Instrumentation, CERN, Geneva (1959), p. 274.
2. I. M. Kapchinskij and A. S. Kronrod, Conference on High Energy Accelerators, Dubna (1963), AEC CONF-114, p. 1241.
3. P. L. Morton, Rev. Sci. Instr. 36, 1826 (1965).
4. R. L. Gluckstern, Proceedings of the 1966 Linear Accelerator Conference, October 3-7, 1966, Los Alamos Scientific Laboratory LA-3609, p. 237.
5. P. M. Lapostolle, CERN Report ISR-300 LIN/66-33, November 8, 1966.
6. T. Nishikawa, SJC-A-67-1, University of Tokyo (June, 1967).
7. S. Ohnuma, Yale Internal Report Y-17 (January, 1967).
8. P. M. Lapostolle, CERN Report ISR-300 LIN/66-32, October 26, 1966.
9. S. Ohnuma, Proceedings of the 1966 Linear Accelerator Conference, October 3-7, 1966, Los Alamos Scientific Laboratory LA-3609, p. 220.
10. R. Chasman, BNL Internal Report AGSCD-31 (February, 1968).
11. D. A. Swenson, K. R. Crandall and J. E. Stovall, private communication (August, 1967 and January, 1968). See also K. R. Crandall, Proceedings of the 1966 Linear Accelerator Conference, October 3-7, 1966, Los Alamos Scientific Laboratory LA-3609, p. 233.
12. B. Chidley, private communication (April, 1968).

13. F. Vermeulen, CERN Report MPS/Int. LIN 67-5 (August, 1967).
14. C. Agritellis and R. Chasman, "Design of a Buncher and the Transport System in its Drift Tube Space for the 200 MeV BNL Injector Linac," published in this volume p.328.
15. Th. J. M. Sluyters and V. J. Kovarik, Proceedings of the Sixth International Conference on High Energy Accelerators, Cambridge, Massachusetts (1967).
16. J. Huguenin et al., Proceedings of the 1966 Linear Accelerator Conference, October 3-7, 1966, Los Alamos Scientific Laboratory LA-3609, p. 355.
17. V. A. Batalin et al., "The I-2 Proton Linear Accelerator," (translation, CERN, 1968).
18. A. Benton, R. Chasman and C. Agritellis, IEEE Trans. Nucl. Sci. NS-14, No. 3, 577 (1967).
19. R. L. Gluckstern, Proceedings of the 1966 Linear Accelerator Conference, October 3-7, 1966, Los Alamos Scientific Laboratory LA-3609, p. 207.
20. S. Ohnuma, *ibid*, p. 214.
21. R. Chasman, *ibid*, p. 224.
22. D. A. Swenson, Bull. Amer. Phys. Soc. 11, 733 (1966). This was an invited paper at the American Physical Society Meeting August 30, 1966, Mexico City.

DISCUSSION

(R. W. Chasman)

VAN STEENBERGEN, NAL-BNL: I get the impression that there is a limit to the goal of obtaining smaller emittances from the preinjector since the resulting higher brightness will lead to a larger blow-up factor in the linac. If I understand your results correctly, one almost approaches a fixed value of emittance for a given current.

CHASMAN, BNL: That is correct. But this impression is true only for these results and their associated assumptions. I believe a definite conclusion cannot be made now. I should mention that the initial charge distributions that I have described were also replaced by gaussian distributions separately, in each of the two transverse planes, and very similar results were obtained.

CURTIS, NAL: You've talked about the emittance blow-up due to non-linear space charge forces and due to coupling with the longitudinal motion. I would like to ask a question about a hypothetical case. Suppose there was zero longitudinal phase space, with a very bright beam. What would happen under these conditions at the beginning of the linac?

CHASMAN, BNL: I have mentioned before that the source of the transverse emittance blow-up comes from both transverse to longitudinal coupling, and the transverse-transverse coupling of the non-linear space-charge forces. I have not yet had time to study the separate contributions of these two coupling terms. If the longitudinal transverse coupling is dominant, then running an infinitely long beam should take away the increase in emittance. But if there is transverse-transverse coupling, it should still be there. This is really one of the tests that must be done yet.

LAPOSTOLLE, CERN: In your numerical computations you used alternating gradient quadrupole focusing, where transverse dimensions oscillate periodically with the factor Ψ . Have you any results which might indicate whether the blow-up found is a function of the amplitude of Ψ ?

CHASMAN, BNL: If one decreases the quadrupole gradient, this would make Ψ smaller, as can be seen from the usual stability diagram. I have performed calculations with lower gradients and have not seen any improvement in the results.

VAN STEENBERGEN, NAL-BNL: One point puzzles me. The emittance blow-up relates to the non-linear terms of the space charge forces. How do you explain the parameter variation with the quadrupole gradient? I assume the quadrupole fields compensate for the linear space charge forces.

CHASMAN, BNL: There are two factors involved here. If you lower the gradients you get closer to the stability limits, so any coupling effect should cause a large emittance growth. On the other hand, if you increase the quadrupole gradients, you might make the non-linear terms larger, since the charge density in physical space becomes larger.

VAN STEENBERGEN, NAL-BNL: This means that one should be able to define new radial stability boundaries by dimensioning the linac parameters so that one remains further removed from the instability boundaries, and thus decrease the effect of coupling on the emittance blow-up.

CHASMAN, BNL: That is the point, though. If the beam is very bright, the effect of brightness of k_t is such as to make it go to zero as the brightness goes up. The selection of the quadrupole gradient, for a given brightness, is a compromise between the two factors I have mentioned. For the brightness that people talk about now, one stays fairly close to the stability limit.

Inj. ENERGY = 0.750 MeV, AVERAGE ACCELERATION = 1 MeV/m,
 $\nu_{RF} = 200$ Mc, $\phi = -32^\circ$, +--+ QUADRUPOLE CONFIGURATION,
 MAGNET LENGTH/CELL LENGTH = 0.5, BORE RADIUS = 1 cm,
 TRANSVERSE EMITTANCE = $I \cdot 22.5 \pi$ cm-mrad (I IN amp.)
 INITIAL ENERGY SPREAD = ± 0.020 MeV.

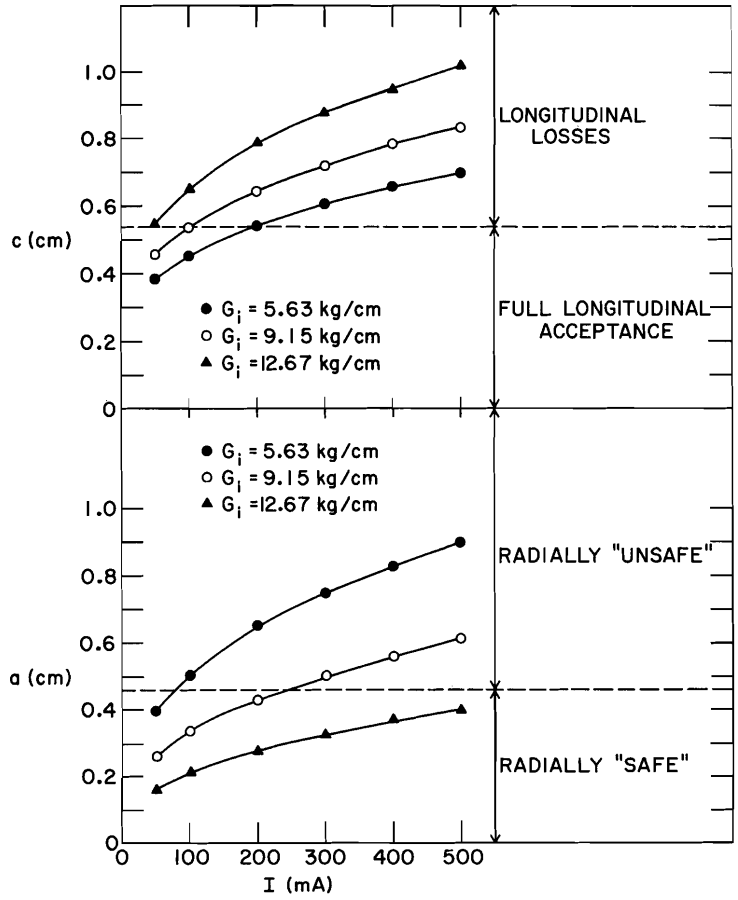


Fig. 1. Transverse and Longitudinal Dimensions (a and c) of a Matched Beam as Functions of Current for Different Initial Quadrupole Gradients.

Inj. ENERGY = 0.750 MeV, AVERAGE ACCELERATION = 1 MeV/m,
 $\nu_{RF} = 200$ Mc, $\phi = -32^\circ$, +--+ QUADRUPOLE CONFIGURATION,
 MAGNET LENGTH/CELL LENGTH = 0.5, BORE RADIUS = 1cm,
 $G_i = 9.15$ kg/cm, INITIAL ENERGY SPREAD = ± 0.020 MeV.

- TRANSVERSE EMITTANCE = $I \cdot 2.25 \pi$ cm-mrad (I IN amp.)
- TRANSVERSE EMITTANCE = $I \cdot 22.5 \pi$ cm-mrad (I IN amp.)
- ▲ TRANSVERSE EMITTANCE = $I \cdot 90.0 \pi$ cm-mrad (I IN amp.)

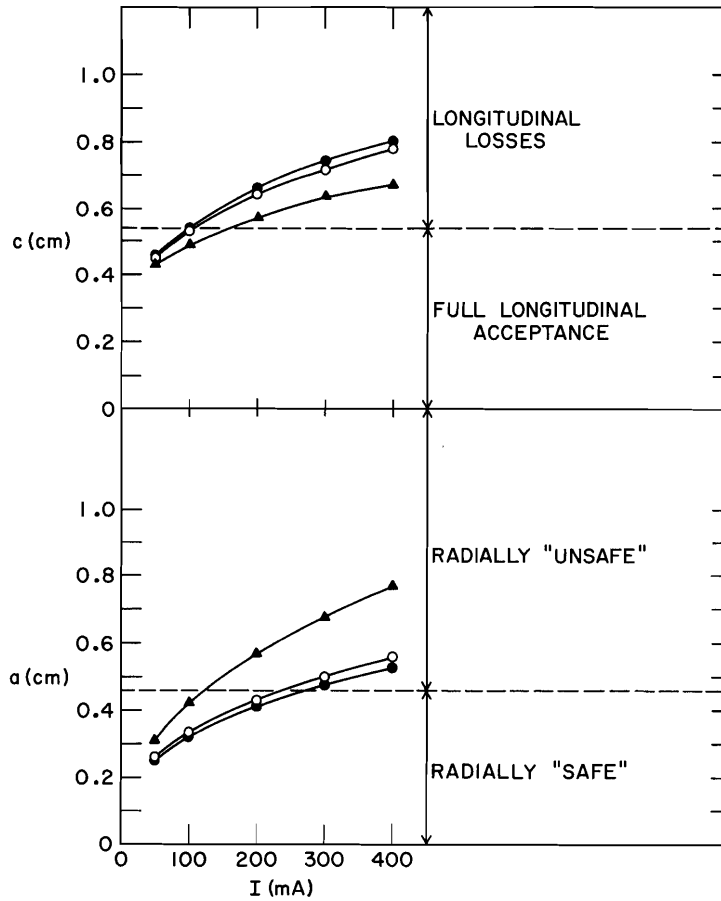


Fig. 2. Transverse and Longitudinal Dimensions (a and c) of a Matched Beam as Function of Current for Different Initial Transverse Emittances.

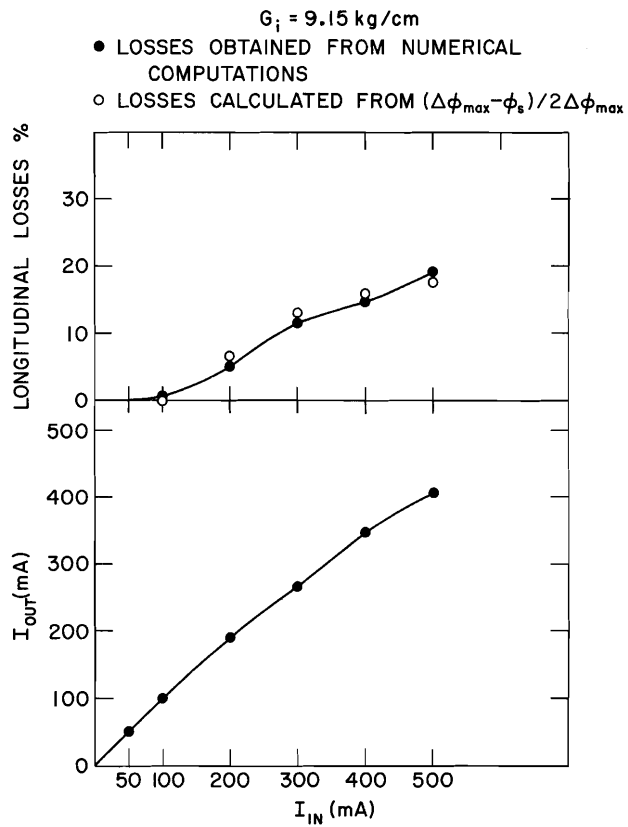


Fig. 3. Output Versus Input Current for an Initial Quadrupole Gradient of 9.15 kG/cm.

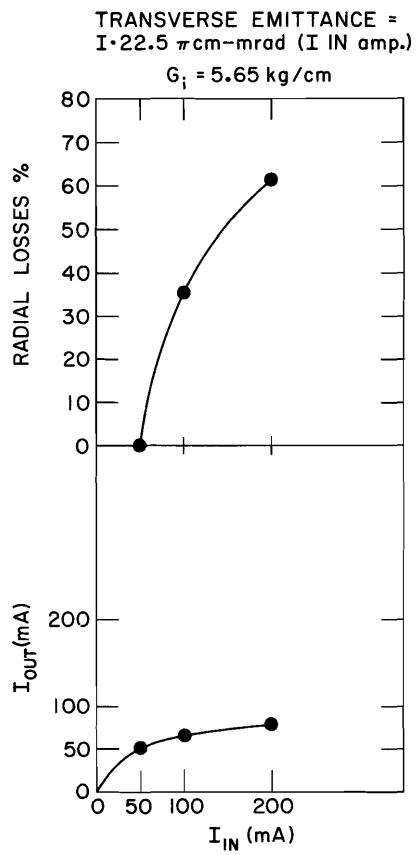
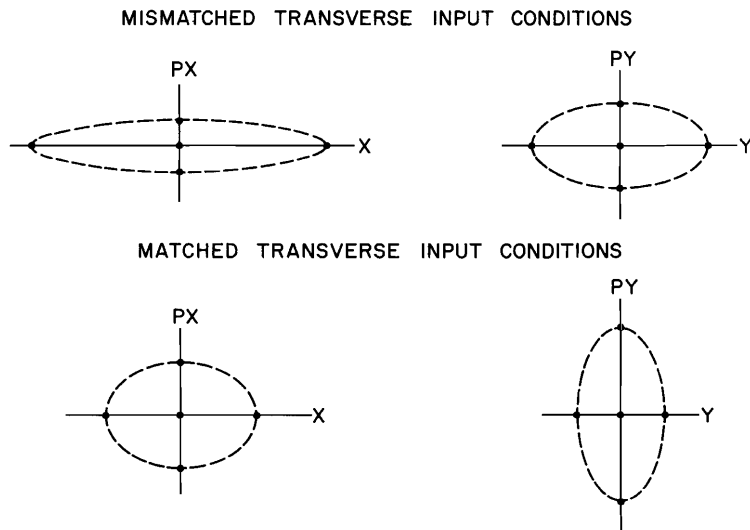


Fig. 4. Output Versus Input Current for an Initial Quadrupole Gradient of 5.63 kG/cm.



INITIAL NORMALIZED EMITTANCE = $0.09 \pi \text{ cm-mrad}$
 $I = 100 \text{ mA}$, $G_s = 9.15 \text{ kg/cm}$
 ● MISMATCHED TRANSVERSE INPUT CONDITIONS
 ○ MATCHED TRANSVERSE INPUT CONDITIONS

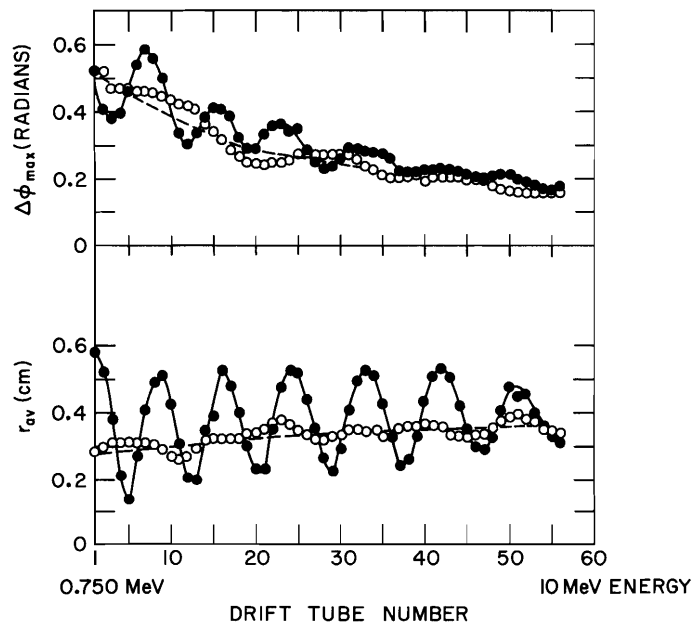


Fig. 5. Transverse and Longitudinal Beam Envelopes as Function of Drift Tube Number of a Transversely Matched and a Transversely Mismatched Beam. (Longitudinal input conditions are those of a perfectly matched beam.)

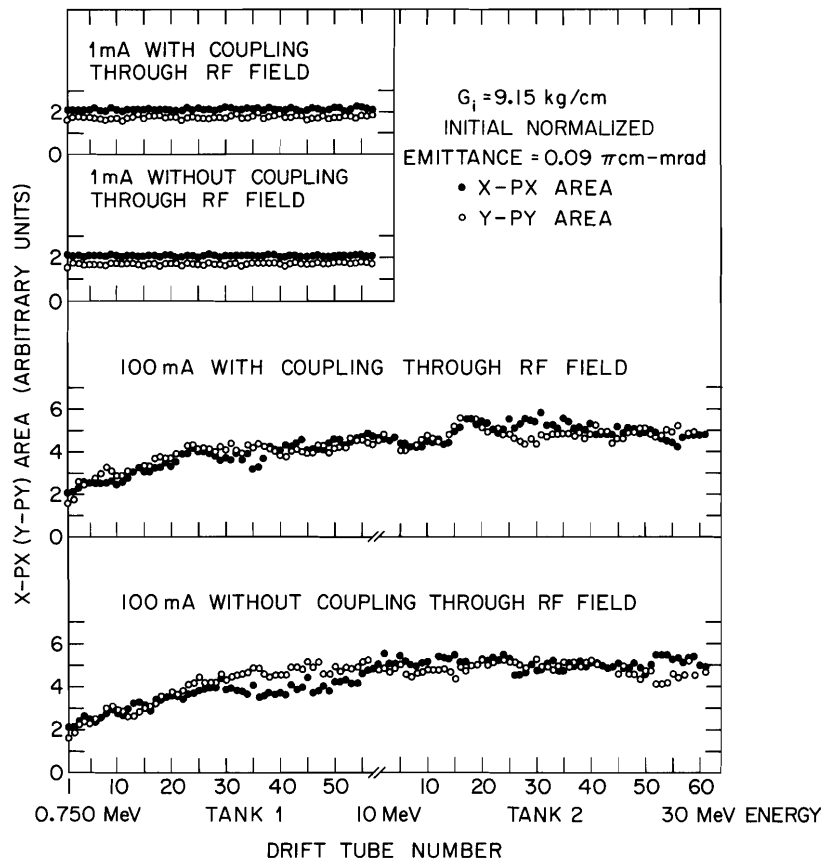


Fig. 6. Transverse Emittances as Function of Drift Tube Number Obtained with and without Coupling through the rf Field for 100 mA and 1 mA. (Input conditions are those of a 100 mA matched beam.)

INITIAL NORMALIZED EMITTANCE = 0.09 π cm-mrad
I = 100 mA, $G_i = 9.15$ kg/cm

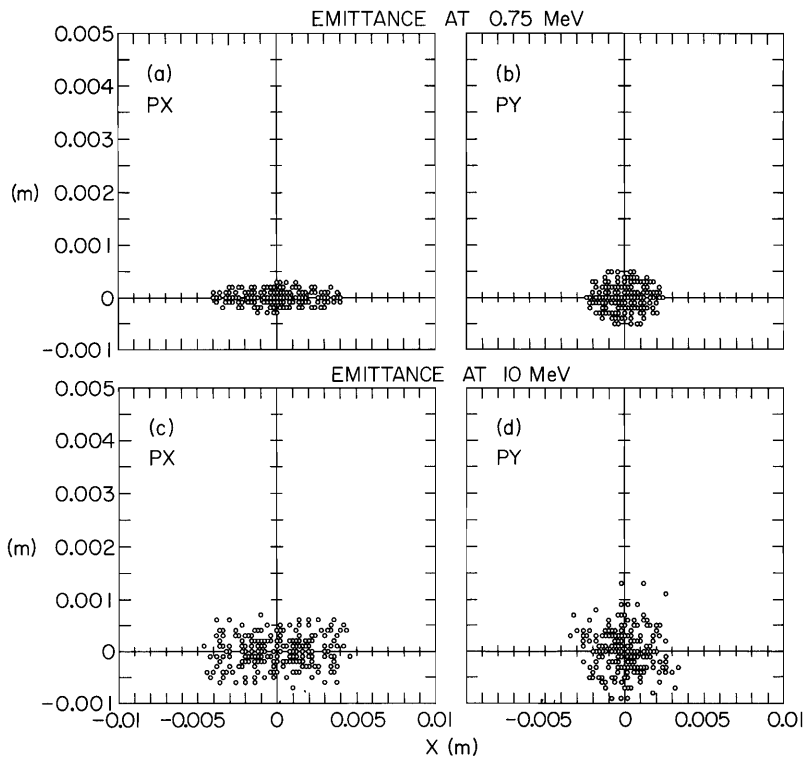


Fig. 7. Particle Distributions in $x-p_x$ and $y-p_y$ Planes, at 0.750 MeV and 10 MeV, Obtained in Run with Coupling through rf Field for 100 mA.

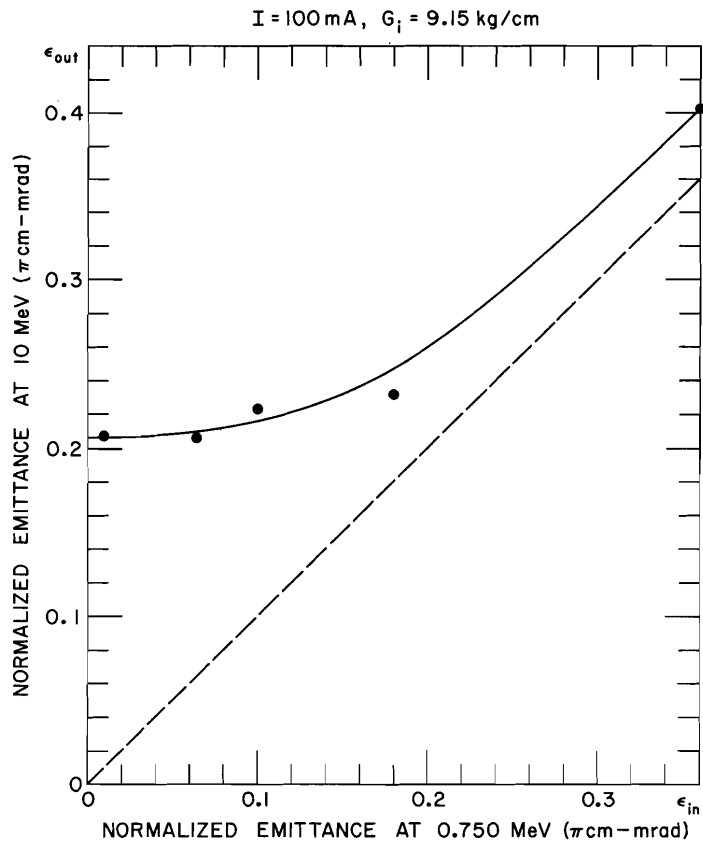


Fig. 8. Normalized Emittance at 10 MeV at Function of Normalized Emittance at 0.750 MeV Obtained for a Beam of 100 mA.

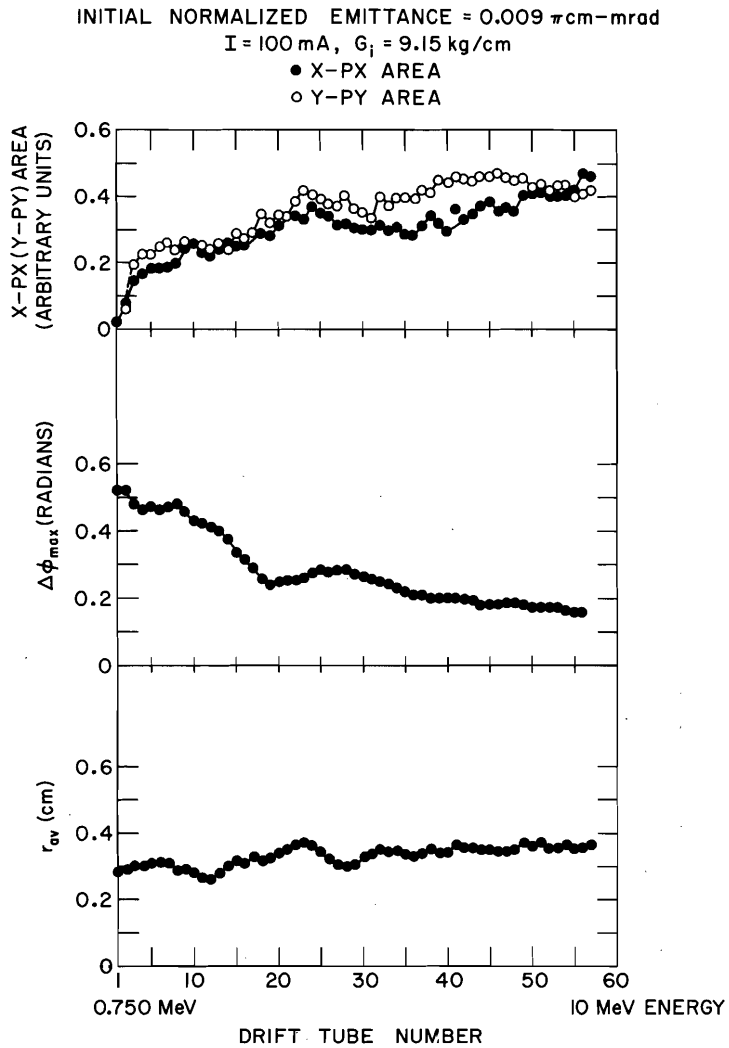


Fig. 9. Transverse and Longitudinal Envelopes and Transverse Emittances as Function of Drift Tube Number for 100 mA and Initial Normalized Emittance of 0.009π cm-mrad.

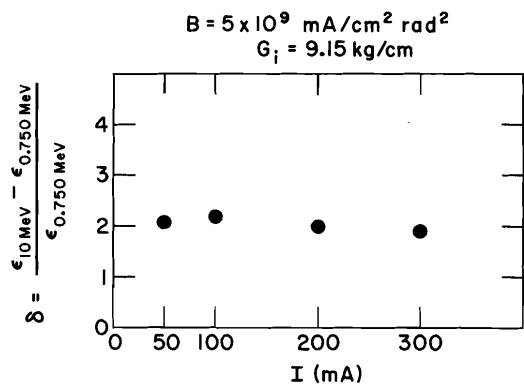


Fig. 10. Fractional Emittance Increase at 10 MeV as Function of Current for a Beam Brightness of $5 \times 10^9 \text{ mA/cm}^2 \text{ rad}^2$.

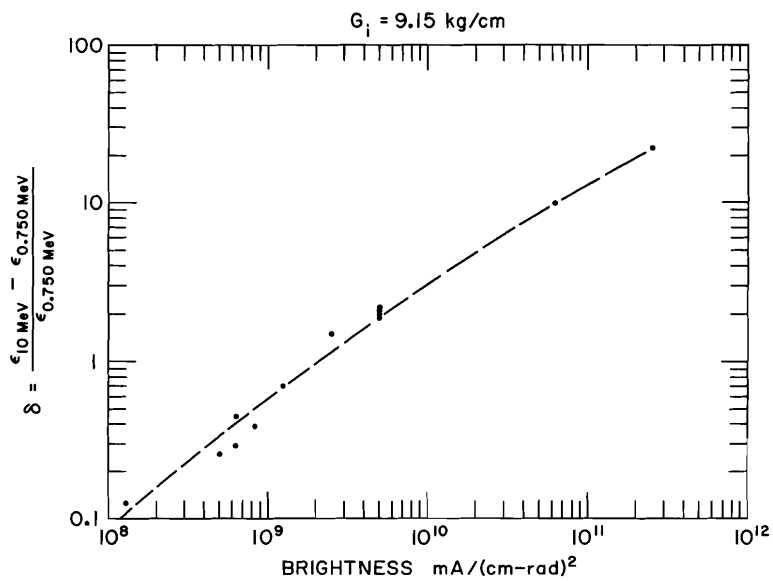


Fig. 11. Fractional Emittance Increase at 10 MeV as Function of Brightness. (Obtained from runs with different currents and different initial emittances)

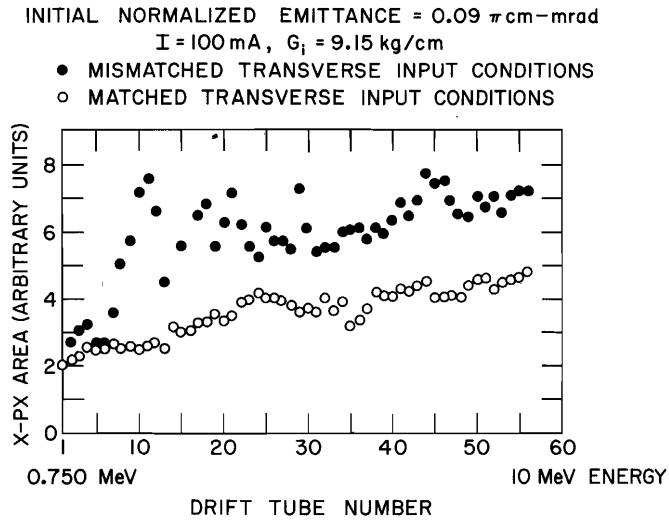


Fig. 12. $x-p_x$ Emittances as Function of Drift Tube Number for a Transversely Matched and a Transversely Mismatched 100 mA Beam. (Longitudinal input conditions are those of a perfectly matched beam.)

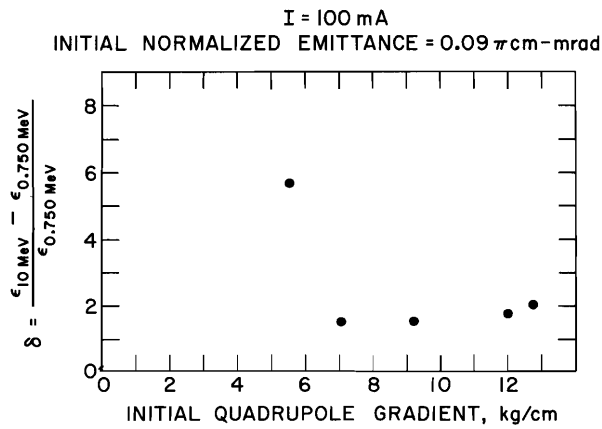


Fig. 13. Fractional Emittance Increase at 10 MeV as Function of Initial Quadrupole Gradient for a Beam of 100 mA and Initial Normalized Emittance of $0.09 \pi \text{ cm-mrads}$.